

LU TP 17-13
May 2017

**Study of Particle Production Mechanisms in PYTHIA 8
using Angular Correlations**

Joakim Alnefjord

Department of Astronomy and Theoretical Physics, Lund University

Bachelor thesis supervised by Torbjörn Sjöstrand



LUND
UNIVERSITY

Abstract

An analysis of two-particle angular correlations was recently performed on measurements taken from pp collisions at $\sqrt{s} = 7$ TeV by ALICE at the LHC. The correlations for mesons are in good agreement with simulations performed in Monte Carlo event generators such as PYTHIA and PHOJET, but there is a significant difference for baryons. We here investigate particle production mechanisms in PYTHIA 8 by studying their effect on the angular correlations for the particles produced. No obvious errors in these mechanisms are found by the study performed in this thesis.

Populärvetenskaplig sammanfattning

En forskargrupp vid partikelacceleratoren Large Hadron Collider (LHC) har nyligen visat att för en viss mätning så stämmer inte data från experiment överens med resultat från datorsimuleringar. Mätningen som gjordes var en undersökning av vinkelrelationer mellan de partiklar som bildas när andra partiklar kollideras vid väldigt hög energi, vilket innebär en hastighet väldigt nära ljusets.

De partiklar som kolliderades var protoner, som är de positivt laddade partiklarna som finns i atomkärnor. Antalet protoner i kärnan bestämmer atomtypen och atomens kemiska egenskaper, exempelvis har syreatomer 8 protoner i kärnan men kolatomer har bara 6 protoner. I kollisionerna bildas det både partiklar som många har hört talas om som protoner och neutroner, som är byggstenar i atomkärnor, men också partiklar som för många är okända som exempelvis pioner och kaoner. Protoner och neutroner tillhör gruppen baryoner. Pioner och kaoner tillhör gruppen mesoner. För mesonerna är skillnaden mellan experiment och simuleringar liten, men för baryonerna är skillnaden större.

Det finns flera möjliga orsaker som skulle kunna förklara skillnaden mellan experiment och teori. Teorin är väldigt komplicerad och därför används approximationer istället. Är dessa approximationer orimliga? Implementeras approximationerna felaktigt i programmet som simulerar kollisioner? Kan det bero på någon felkälla i analysen av experimentell data? PYTHIA, som är ett vanligt använt simuleringsprogram, stämmer väl överens med experiment på många andra sätt, men inte just i det här fallet. Syftet med denna rapport är att fokusera på programmet för att kunna undersöka specifika delar av teorin individuellt. Detta för att försöka förstå de processer som kan tänkas leda till denna skillnad. Förhoppningsvis kan detta i framtiden leda till att problemet blir löst.

Contents

| | | |
|----------|---|-----------|
| 1 | Introduction | 3 |
| 2 | Background | 3 |
| 2.1 | Hadronic structure | 3 |
| 2.2 | Lund string model and hadronization | 4 |
| 2.3 | Coordinate system | 6 |
| 3 | Correlation function | 7 |
| 3.1 | Sources of correlations | 8 |
| 4 | The problem | 9 |
| 5 | Analysis | 10 |
| 5.1 | Simple strings | 10 |
| 5.2 | Cuts and particle distributions | 15 |
| 5.3 | Individual particle production mechanisms | 17 |
| 6 | Conclusions | 19 |

1 Introduction

A recent analysis of measurements, taken from pp collisions at $\sqrt{s} = 7$ TeV, made by the ALICE collaboration at the LHC [1], showed that two-particle angular correlations for mesons are in good agreement with Monte Carlo event generators such as PYTHIA and PHOJET, but there is a significant difference for baryons.

The aim of this study is to investigate particle production mechanisms in PYTHIA 8 by looking at the angular correlations for the particles produced. The problem can be investigated from two starting points. One of them is to begin at the top and then remove individual mechanisms to see what their effect is on the angular correlation. The other is to begin with the simplest case and then add new layers of complexity. The simplest case here is a single $q\bar{q}$ pair, connected with a Lund model string, where the quark and the antiquark are scattered in opposite directions. This makes it possible to study the hadronization process at the lowest level. These will both be used as aid to understand the mechanisms involved. Hopefully this increased understanding may in the future lead to a solution to the problem.

The structure of this thesis is quite straightforward. The theoretical background is given in section 2, including a description of the Lund String Model, the hadronization process, and choice of coordinate system. The properties of the correlation function and how particle production mechanisms give rise to correlations are discussed in section 3. The problem itself is described and displayed in the form of angular correlation plots in section 4. Section 5 contains the analysis of the results from simulations. Finally, a summary and conclusion is given in section 6, which also includes a discussion on how to continue from here.

2 Background

2.1 Hadronic structure

Hadrons are bound states of quarks and/or antiquarks. The hadrons consist of a number of valence quarks, a sea of gluons, and multiple quark-antiquark pairs. The baryons are the hadrons which consist of three quarks, the anti-baryons of three anti-quarks, and the mesons of a quark and an anti-quark, not necessarily of the same type. Although the valence quarks remain the same, the sea is constantly changing due to random fluctuations that cause quark-antiquark pairs to be spontaneously created and annihilated as well as gluons being emitted and reabsorbed by other quarks and gluons, which are commonly referred to as partons.

In particular, the protons consist of the three valence quarks: up, up, and down. When protons collide at high energy in particle accelerators a parton from one proton can scatter against a parton from the colliding proton. An example of this type of scattering is shown in figure 1a. This figure shows a Feynman diagram [2] of the quark scattering including the colour flow between the two quarks, where a blue quark scatters against a red quark via either a $r\bar{b}$ or a $b\bar{r}$ virtual gluon. Because of the random fluctuations, however, the scattered partons are not necessarily only up or down quarks. It is possible for other types of quarks or gluons to be scattered. The two colliding partons are scattered in opposite directions while the proton remnants continue relatively unaffected along the beam paths. Figure 1b shows how so called strings connect scattered quarks to the diquark remnants, which can

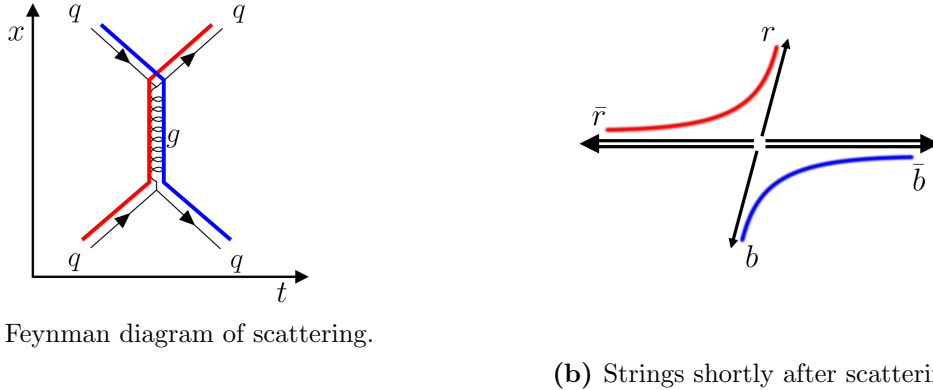


Figure 1: Colour flow in a common $qq \rightarrow qq$ scattering. (a) shows the Feynman diagram for this event, including the colour flow between the two quarks. (b) shows a spatial snapshot of two strings connected between a scattered quark and a proton remnant.

be seen as collectively having an anticolour that matches the colour of the scattered quark to form the initial colourless state. Technically, the scattered partons only leave the point of collision in opposite directions in their rest frame. In the lab frame, however, they are longitudinally boosted and not necessarily moving away in exactly opposite directions. The Lund String Model, describing the hadronization process after the collision, is explained in the next section.

2.2 Lund string model and hadronization

This section contains a summary of relevant parts in ref. [3], where a more detailed description can be found. Quarks are confined in colourless states known as hadrons. Attempts to knock a quark out of its bound hadronic state will result in a narrow tube, or string, of non-perturbative gluons being formed between the quark and the remnant of the hadron. The amount of energy per length it takes to extend this string is approximately 1 GeV/fm. The string can spontaneously break in multiple, causally disconnected, places by creating quark-antiquark pairs, thereby producing two or more colourless hadrons. A commonly used description of this process is the Lund Model.

In the type of process shown in figure 1a, two quarks would be scattered opposite to each other, which means that the newly formed hadrons will appear as opposing jets in a detector. These hadrons are created along the curved blue and red strings shown in figure 1b. The majority of the particles are produced in the directions of either the beam axis or the scattered quark. For this type of mechanism mostly up, down, and strange quark-antiquark pairs are created when the string breaks, with the ratio ($u : d : s : c \approx 1 : 1 : 0.3 : 10^{-11}$). The creation of heavier quarks is strongly suppressed due to tunnelling effects [4]. Pairs of diquarks, e.g. $us-\bar{u}\bar{s}$ or $ds-\bar{d}\bar{s}$, may also be created, which allows for the production of baryons.

A meson can be represented by the spacetime diagrams in figure 2, where figure 2a shows the meson at rest and figure 2b shows the meson in a reference frame where it is in motion. In this figure, the quark and the antiquark begin their oscillation by moving away from each other

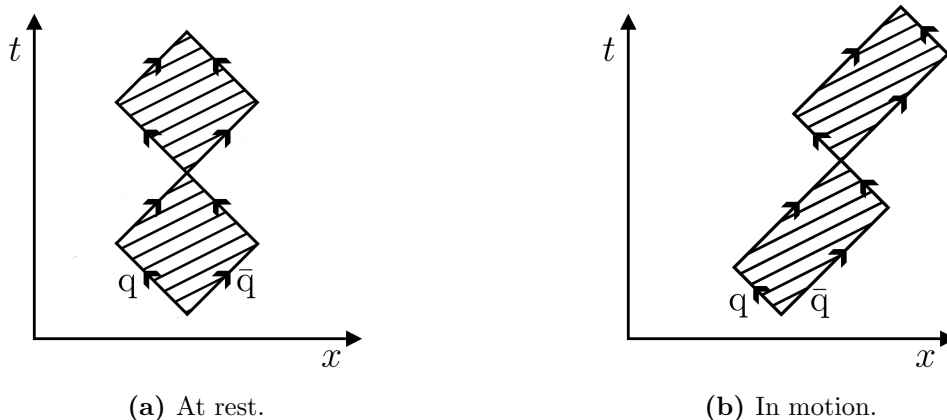


Figure 2: Spacetime diagram of a meson with its oscillating $q\bar{q}$ pair. Note that the axes are swapped compared to figure 1a.

at approximately the speed of light, since their masses are small compared to the energies involved. The kinetic energy of the quarks is converted to potential energy in the string that connects them. This continues until the quarks reach zero kinetic energy, at which point the direction is reversed and the potential energy is converted into kinetic energy. The area that the string sweeps in these diagrams is shown as parallel lines between the quarks.

The hadronization process can be visualized by an example in figure 3 below. For this example, a quark and an antiquark are scattered in opposite directions with a string connecting them. Instead of oscillating, the string breaks, in this case in three places, to form quark-antiquark pairs. This leads to four new hadrons being produced, seen in figure 3a as the four sections of rectangles connected corner to corner, labelled P_1 , P_2 , P_3 and P_4 . On average, the breaks occur after a certain invariant time τ . This means that they will generally occur near the hyperbola $\tau^2 = t^2 - x^2$, where τ^2 is a constant, if the collision event is set at coordinates $(0, 0)$.

The process described above can also be seen as a long string broken down into smaller pieces, as demonstrated in figure 3b, where specific $q\bar{q}$ pairs have been chosen as an example. In this particular case u and \bar{u} are scattered in opposite directions. Three $q\bar{q}$ pairs are independently created when the string breaks, forming the four mesons: π^0 , π^+ , K^0 , K^- . This type of hadronization from a string also involves quark pairs being created with opposite transverse momenta, thus contributing to the spread of the hadrons within jets. This process is displayed in figure 3c below, where the magnitudes of the arrows indicate the magnitudes of the transverse momenta. Figures 3a, 3b, and 3c all display the same event, but are split up into multiple simple figures to avoid a single cluttered and complicated figure.

A pp collision does not necessarily consist of a single parton-parton collision, there may be multiple parton interactions (MPIs) where multiple parton pairs are scattered, independent of each other. All partons may also emit bremsstrahlung in the form of gluons, which may then create $q\bar{q}$ pairs, either before the hard interaction as initial state radiation (ISR) or after as final state radiation (FSR). MPIs, ISR, and FSR increase the spread of partons and therefore increase the spread of particles created in a hadron collision. In addition to particles being

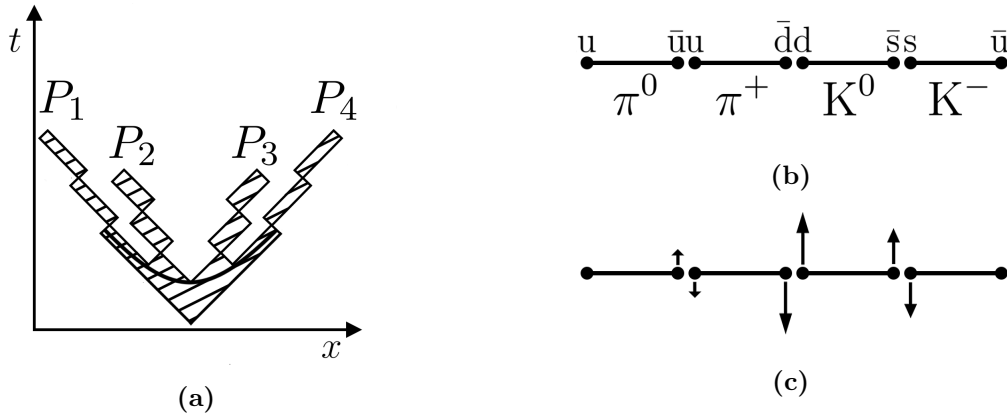


Figure 3: A hadronization process displayed in the form of a spacetime diagram in (a) and as the fragmentation of a string in (b) and (c). In (b), specific $q\bar{q}$ pairs are given as an example, leading to the production of the four mesons: π^0 , π^+ , K^0 , and K^- . In (c), the transverse motion of the created $q\bar{q}$ pairs is displayed.

created directly when a string breaks, particles may also be produced indirectly via decays of other particles.

2.3 Coordinate system

Instead of expressing the particle's direction of motion using the Euclidian coordinates p_x , p_y and p_z , a different set of coordinates is commonly used e.g. at the LHC. The motion in the transverse plane to the beam axis is given by a transverse momentum p_T and an azimuthal angle φ . The motion along the beam axis is given by the rapidity y . A useful property of these coordinates is the invariance of difference in rapidity under Lorentz boosts to a primed reference frame along the direction of the incoming particle beam, ($\Delta y' = \Delta y$, $\varphi' = \varphi$, $p'_T = p_T$). The invariance of φ and p_T is clear since Lorentz boosts do not affect coordinates transverse to the direction of the boost. The invariance of difference in rapidity may easily be shown with the definition of rapidity (eq. 2.1) and a Lorentz boost (eq. 2.2).

$$y = \frac{1}{2} \ln \frac{E + p_z}{E - p_z} \quad (2.1)$$

$$\mathbf{P}' = \begin{pmatrix} E' \\ p'_x \\ p'_y \\ p'_z \end{pmatrix} = \begin{pmatrix} \gamma & 0 & 0 & -\beta\gamma \\ 0 & 1 & 0 & 0 \\ 0 & 0 & 1 & 0 \\ -\beta\gamma & 0 & 0 & \gamma \end{pmatrix} \begin{pmatrix} E \\ p_x \\ p_y \\ p_z \end{pmatrix} = \mathbf{\Lambda} \mathbf{P}. \quad (2.2)$$

In equation 2.1, y is the rapidity, E is the total energy of the particle, and p_z is the z-component of its momentum. Equation 2.2 shows the Lorentz boosted four-vector \mathbf{P}' , the Lorentz transformation matrix $\mathbf{\Lambda}$ for a boost in the z-direction, and the original four-vector \mathbf{P} . If the mass of the particle is small relative to its momentum, or if the mass is simply not known, the approximation $E \approx |\vec{p}| = p$ can be used. Thus, a pseudorapidity η can be expressed as a function of the polar angle θ ,

$$\eta = \frac{1}{2} \ln \frac{p + p_z}{p - p_z} = \frac{1}{2} \ln \frac{p(1 + \cos\theta)}{p(1 - \cos\theta)} = \frac{1}{2} \ln \frac{2 \cos^2 \frac{\theta}{2}}{2 \sin^2 \frac{\theta}{2}} = -\ln \left[\tan \frac{\theta}{2} \right]. \quad (2.3)$$

In addition to this, there is also a rotational invariance in differences of azimuthal angle, ($y' = y$, $\Delta\varphi' = \Delta\varphi$, $p'_T = p_T$).

3 Correlation function

The correlation between particles is calculated by considering e.g. the difference in pseudorapidity and difference in azimuthal angle between pairs of particles. Different phenomena give different characteristic distributions in this $(\Delta\eta, \Delta\varphi)$ -space, and the sum of all effects gives the final shape of the correlation function. For the correlation functions described in this section, a value of unity corresponds to vanishing correlation, a value greater than unity corresponds to positive correlation, and a value less than unity corresponds to negative correlation. In general, the correlation function for pairs of particles can be defined as

$$C(\varphi_1, \varphi_2, \eta_1, \eta_2) = \frac{P_{12}(\varphi_1, \varphi_2, \eta_1, \eta_2)}{P_1(\varphi_1, \eta_1) P_2(\varphi_2, \eta_2)}. \quad (3.4)$$

Here, P_{12} is the probability of finding the two particles at (φ_1, η_1) and (φ_2, η_2) respectively. Similarly, P_1 and P_2 are the probabilities of finding one particle with a certain φ and η independent of the other particles in the event. It is more convenient, however, to use $\Delta\varphi$ and $\Delta\eta$ as arguments for the correlation function since they leave the correlation function invariant under Lorentz boosts along the beam path and rotations around the beam path. Applying this, it is possible to construct a correlation function as

$$C(\Delta\varphi, \Delta\eta) = \frac{S(\Delta\varphi, \Delta\eta)}{B(\Delta\varphi, \Delta\eta)}, \quad (3.5)$$

where $S(\Delta\varphi, \Delta\eta)$ is a signal function and $B(\Delta\varphi, \Delta\eta)$ is a background function, given by

$$S(\Delta\varphi, \Delta\eta) = \frac{1}{N_{S(tot)}} \frac{d^2 N_S}{d(\Delta\varphi) d(\Delta\eta)} \quad \text{and} \quad (3.6)$$

$$B(\Delta\varphi, \Delta\eta) = \frac{1}{N_{B(tot)}} \frac{d^2 N_B}{d(\Delta\varphi) d(\Delta\eta)}. \quad (3.7)$$

For the signal function $S(\Delta\varphi, \Delta\eta)$, the number of signal pairs N_S in a region $d(\Delta\varphi) d(\Delta\eta)$ is divided by the total number of signal pairs $N_{S(tot)}$, and similarly for the background function $B(\Delta\varphi, \Delta\eta)$ where background pairs are used instead. The signal pairs are chosen from the same event and the background pairs are chosen from different events, so that any possible background correlation can be divided out of the signal function, so that what remains is the correlation function $C(\Delta\varphi, \Delta\eta)$. This thesis primarily concerns the correlation of particle pairs in $(\Delta\varphi)$ -space. Since particles are created uniformly in the region of azimuthal angle $0 < \varphi \leq 2\pi$, $B(\Delta\varphi)$ will be equal to 1. Because of this, we can restrict $\Delta\varphi$ by only looking at the absolute value and applying the condition that if $\Delta\varphi > \pi$, then $\Delta\varphi \rightarrow 2\pi - \Delta\varphi$, which means that $\Delta\varphi \in [0, \pi]$. Therefore, the commonly used correlation function in this thesis is simply

$$C(\Delta\varphi) = \frac{\pi}{N_{S(tot)}} \frac{dN_S}{d(\Delta\varphi)}, \quad (3.8)$$

which is proportional to the probability of finding a particle pair with a certain $\Delta\varphi$ but normalized by multiplying by the width of the interval, π , since this is the maximum difference in azimuthal angle between two particles. The normalization is there so that a value of 1 for $C(\Delta\varphi)$ corresponds to zero correlation.

3.1 Sources of correlations

It is important to remember the aspect of randomness in quantum mechanics, and therefore in particle physics, which means that the effects discussed here will not appear as sharp peaks in the correlation function, but rather smeared out like hills. The partons are bound in the proton whose radius r is approximately 1 fm. Together with the lower limit of the Heisenberg uncertainty principle, $\Delta r \Delta p \gtrsim \hbar$, this gives a minimum uncertainty for the momentum p of a parton around 200 MeV ($\hbar = 197$ MeV fm). Incoming partons may then have a slight transverse momentum, known as primordial transverse momentum, which means that outgoing partons will generally not be completely anti-parallel. This effect is then expected to lead to some smearing of the correlation peak around $\Delta\varphi = \pi$. It is also the cause of the transverse momentum kicks in figure 3c, where the quarks are confined within the radius of the string.

In a single hadron collision, there may be MPIs, ISR, and FSR, which all influence the correlation function. MPIs increase the number of uncorrelated parton scatterings, thereby increasing the spread of particles in an event. ISR and FSR may increase the number of jets from a single scattering by emitting gluons, and in that way, increase the spread of particles. These types of phenomena are then all expected to flatten the correlation function.

Decays of particles also influence the correlation function, but not in the same way as MPIs, ISR, and FSR. The contribution in correlation is specific to the exact type and context of a decay. As an example, a particle with high p_T may decay into two low momenta particles, in the rest frame of the mother particle. If this is the case, the transverse boost will make the two daughter particles move in almost the same direction as the mother particle, and will therefore contribute to a peak around $\Delta\varphi = 0$ in the correlation function for this particle pair. If the case is reversed, however, and a low p_T particle decays into two higher p_T particles, the decay may instead contribute with a peak around $\Delta\varphi = \pi$. Correlation may also arise from cases where either one or both of two particles formed next to each other decay, e.g. a π^+ and a ρ^0 which then decays to a π^+ and a π^- , or two ρ^0 mesons which both decay into a $\pi^+\pi^-$ pair.

The string breaks by creating $q\bar{q}$ or $qq\bar{q}\bar{q}$ pairs, which means that the only possibility for two identical particles to be created right next to each other on a fragmenting string is if they are their own anti-particles. For charged pions and kaons, protons, and lambda baryons, which are the particles studied in this thesis, the particles and anti-particles are different. Two π^+ mesons, for example, cannot be created right next to each other since this would violate local charge conservation. The same applies for two same-sign baryons as this would violate local baryon number conservation. The only possibility, for two identical particles to be created right next to each other when the string breaks, is for meson states that are linear combinations of same flavour $q\bar{q}$ pairs, $a u\bar{u} + b d\bar{d} + c s\bar{s} + \dots$, such as the π^0 , η , and ϕ mesons. Therefore the same-sign pairs will get no contributions in correlation directly from the opposite transverse momentum of the quark pair that splits the string, but may get contributions from being created in the same jet.

The number of particles created in each event is also relevant. Events where only a single pair of a given kind is created will produce a strong anti-correlation, due to the local

conservation of strangeness¹, charge, momentum, and baryon number. However, in an event where there are dozens of pairs, these pairs may have different origins and therefore not be as strongly correlated. This means that particles that are generally produced in large amounts in a single event, like π -mesons, will have less pronounced, i.e. more flat correlation functions than particles that are generally produced in small amounts in a single event, like Λ -baryons.

4 The problem

The analysis by the ALICE collaboration was made on data from pp collisions collected with minimum bias at $\sqrt{s} = 7$ TeV. Minimum bias in short means to study all inelastic events, without a selective bias towards a particular type of event. The particles that were studied were pions, kaons, protons, and lambda baryons. The correlation function was therefore calculated for pairs of pions, kaons, protons, and lambda baryons, of both equal and opposite sign: $\pi^+\pi^-$, $\pi^+\pi^+ + \pi^-\pi^-$, $p\bar{p}$, $pp + \bar{p}\bar{p}$, et cetera. The cuts given in table 1, taken from ref. [1], defines the range of particles studied. Introducing these cuts means that we only look at particles in the central region of the detector. The cuts were chosen to maximize the purity of the sample studied by minimizing the number of misidentified particles. In addition to the cuts in table 1, when comparing pairs of particles, another requirement was that $|\Delta\eta| < 1.3$.

Table 1: Cuts in pseudorapidity η and transverse momentum p_T for the four particles, (π , K, p, Λ)

| Particle | Maximum η | Maximum p_T (GeV) | Minimum p_T (GeV) |
|-----------|----------------|---------------------|---------------------|
| π | 0.8 | 2.5 | 0.2 |
| K | 0.8 | 2.5 | 0.3 |
| p | 0.8 | 2.5 | 0.5 |
| Λ | 0.8 | 2.5 | 0.6 |

The corresponding simulation has in this thesis been performed in PYTHIA 8 (version 8.223) [5], and the same applies to all following simulations. The cuts in table 1, together with $|\Delta\eta| < 1.3$, define the simulation “Baseline” in the correlation figures, and apply to all simulations discussed in this thesis unless any changes are explicitly stated. The experimental data including error bars has been read manually, but as accurately as possible, off the PDF-file of Ref. [1] and do therefore not exactly represent the actual experimental data. Any human error expected when data points are read manually has not been explicitly added to the error bars, but is estimated to be relatively small.

In figures 4 and 5 it is clear that PYTHIA 8 is in good agreement with experimental data for the mesons π and K, but we notice a clear difference for the baryons p and Λ . Simulations seem to overestimate the correlation around $\Delta\varphi = 0$ for both the different-sign baryons ($p\bar{p}$, $\Lambda\bar{\Lambda}$), and the same-sign baryons ($pp + \bar{p}\bar{p}$, $\Lambda\Lambda + \bar{\Lambda}\bar{\Lambda}$). The cause of this difference is currently unknown, and the aim of the remaining part of this thesis is to gain understanding about how particle production mechanisms affect these angular correlations.

¹Strangeness conservation may of course be violated by the weak interaction but the timescale for this process is much larger than for the strong interactions.

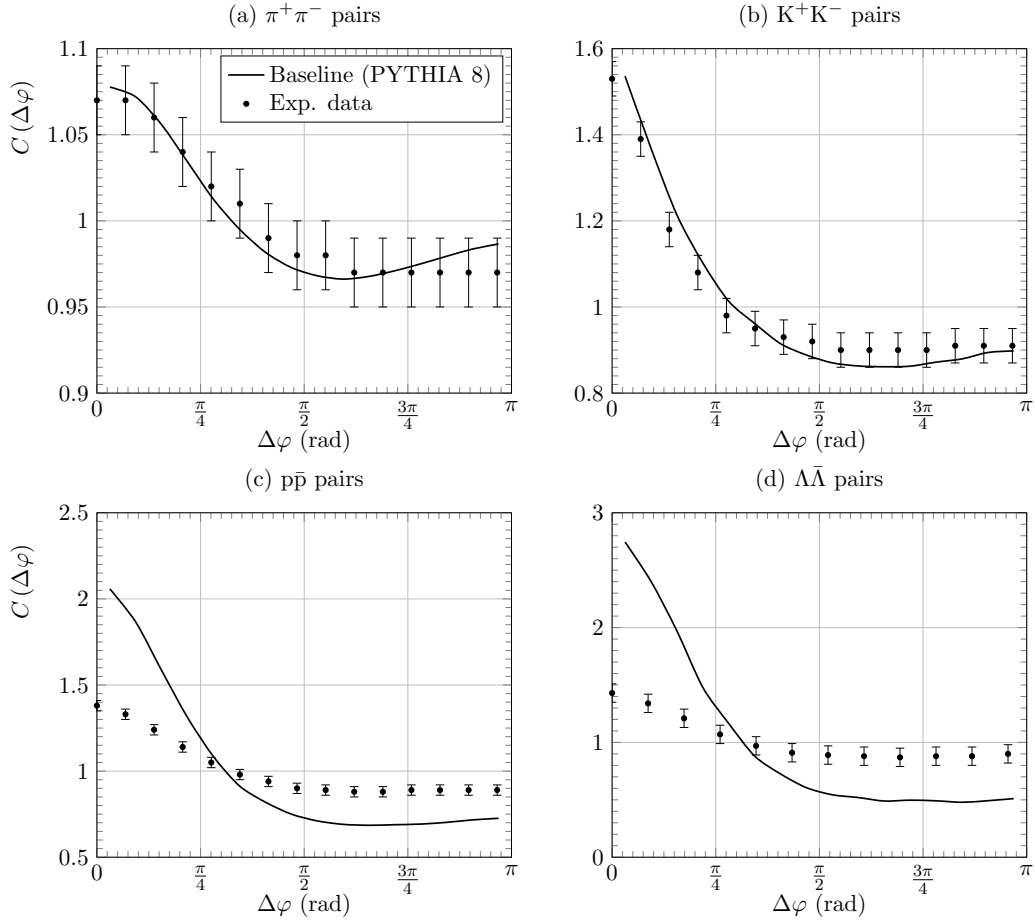


Figure 4: Comparison between simulations (PYTHIA 8) and experimental data of angular correlations for different-sign particle pairs produced in pp collisions at $\sqrt{s} = 7$ TeV. Notice the different scales on the vertical axes.

5 Analysis

5.1 Simple strings

Here, the event is built from the ground up. Instead of colliding protons at $\sqrt{s} = 7$ TeV, specific quarks connected by a string are created and scattered in opposite directions to have more control over the hadronization process. For all events in this section, a u and \bar{u} are connected with a string and scattered in opposite directions with a momentum of 100 GeV each. This energy was chosen arbitrarily, and although being quite high, the energy chosen has a relatively small effect on general shape of the correlation functions and mostly alters the scale of the vertical axis. We here study angular correlations of the particles produced when the string breaks down.

Figures 6 and 7 shows correlation functions created from events where a u and \bar{u} are scattered in opposite directions along the z -axis, which is the beam axis. The string is placed along the z -axis so that we can study the effects of the opposite transverse momenta of the quark pairs that are created when the string breaks. The source of the peak around $\Delta\varphi = \pi$, in the

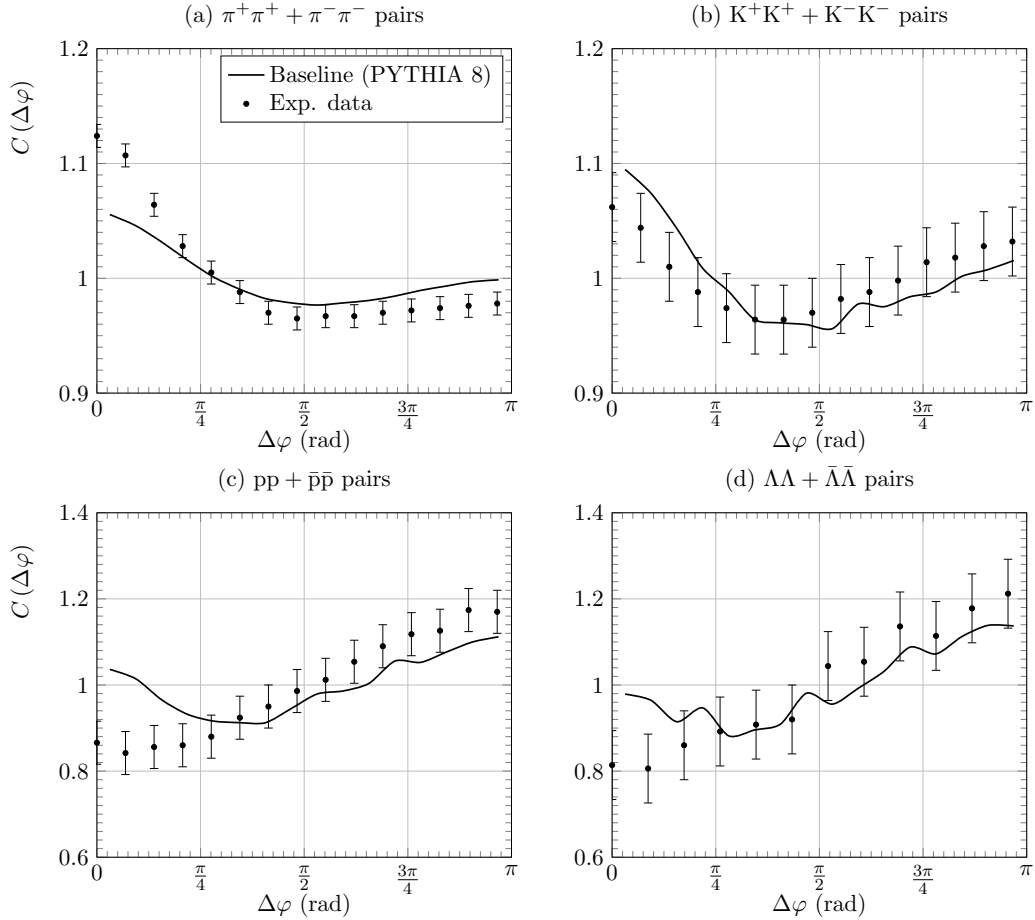


Figure 5: Comparison between simulations (PYTHIA 8) and experimental data of angular correlations for same-sign particle pairs produced in pp collisions at $\sqrt{s} = 7$ TeV.

different-sign plots (a) to (d), originates from the conservation of momentum in the transverse kicks created when $q\bar{q}$ pairs are formed. These different-sign particle pairs are often created right next to each other when the string hadronizes, and since the $q\bar{q}$ pair, which splits the string into the two particles, will be split into opposite directions in the transverse plane, the two particles will often also be created in opposite directions. Removing the possibility of particle decay isolates this phenomenon and amplifies the correlation function.

The same-sign particle correlations look different since same-sign pairs of pions, kaons, protons, and lambda baryons cannot be created right next to each other along a hadronizing string. Same-sign hadrons that come directly from the string will therefore be uncorrelated. This reasoning is made clear by removing the possibility to decay which flattens the angular correlations for the same-sign mesons.

Heavier mesons or baryons whose decay products include charged pions or kaons, however, can be created right next to each other, or next to a charged pion or kaon. They are more likely to be created with opposite transverse momenta which, when they decay, therefore often produce pairs of same-sign pions and kaons created opposite each other in the trans-

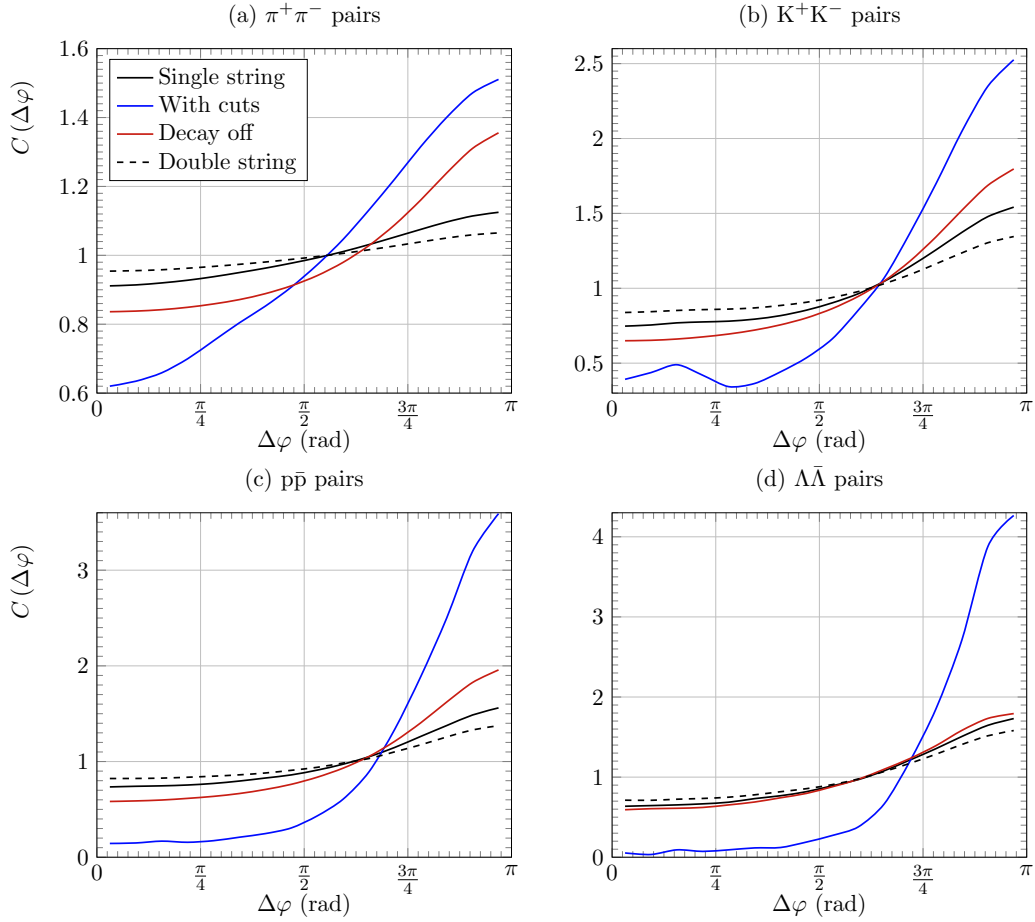


Figure 6: Angular correlations for different-sign particle pairs created from simple strings in the z -direction.

verse plane. An example of this is an event where a ρ^0 meson, which commonly decays to a $\pi^+\pi^-$ pair, is created next to a π^+ meson. The two daughter particles must conserve the momentum of the mother particle, which means that the π^+ that was formed on the string is often created in the opposite transverse direction to the π^+ that was formed in the decay. We could also have two ρ^0 mesons created next to each other on the string. If they both decay to a $\pi^+\pi^-$ pair, then same-sign meson pairs are likely to be created in opposite transverse directions.

The same arguments as previously mentioned in this section also apply if the cuts in table 1 are introduced, however, here the correlation functions are amplified. Adding cuts means only accepting particles with a low η , ($|\eta| < 0.8$), which means that we only look at particles produced close to the centre of the string. For the particles in this narrow range, the effect of opposite- p_T $q\bar{q}$ pairs, that split the string, is highlighted as an increased anti-correlation. The same-sign baryons have been left out in figure 7 due to the difficulty of gathering statistics on these types of events.

Creation of two strings in the same event, either with the two u quarks being scattered

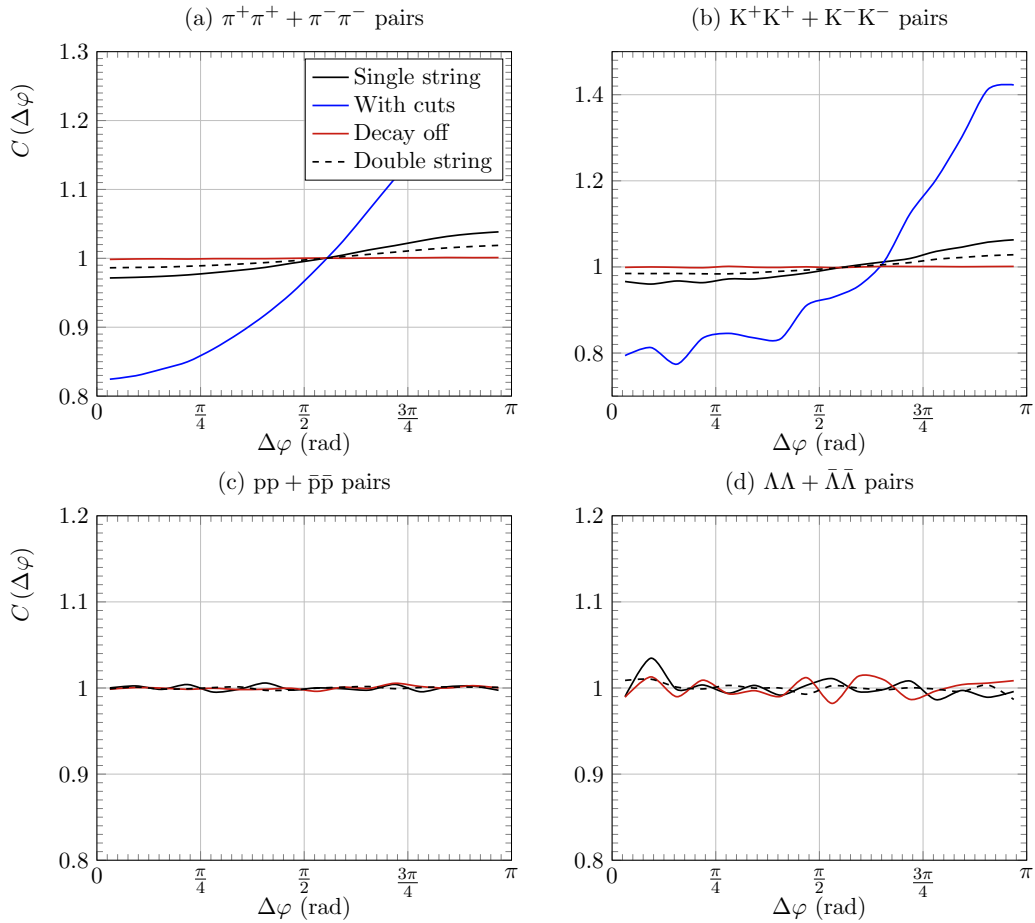


Figure 7: Angular correlations for same-sign particle pairs created from simple strings in the z -direction. For the case with cuts, the same-sign baryons have been left out due to the difficulty of gathering statistics on these types of events.

in the same arbitrarily chosen right direction (RR) or in opposite directions (RL), both contribute with the same effect which is to flatten the correlation function. Regular particles are slightly more often created in the same direction as the u quark, while antiparticles are slightly more often created in the same direction as the \bar{u} quark. The correlation function is only influenced by the particles' transverse motion, however, which makes it independent of the string directions. The correlation function is flattened because including multiple strings allows for a greater number of uncorrelated pairs. Since the two possibilities of having the strings in the same direction or in different directions give the same contributions, only one of them is shown in figures 6 and 7.

Figures 8 and 9 show almost the same scenario as above, except that the u and \bar{u} quarks were scattered in opposite directions in the transverse plane to form two high- p_T jets. This is to study conservation laws in jets. Here we see that the correlation for the different-sign particle pairs is higher around $\Delta\varphi = 0$ than around π . The plots for when decays are turned off are not shown because they are almost identical to the single string plot. This means that the increased peak around $\Delta\varphi = 0$ is mainly because of the tendency for these different-sign

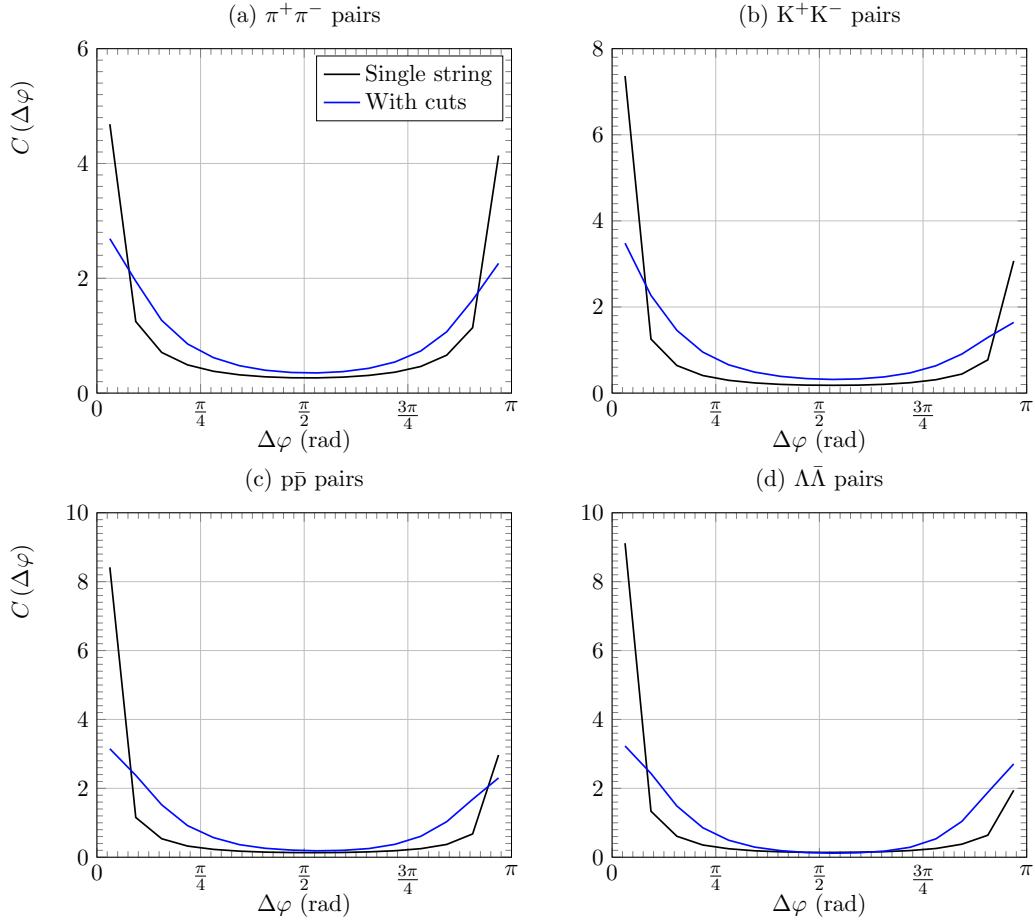


Figure 8: Angular correlations for different-sign particle pairs created from simple strings in the transverse plane.

pairs to be created next to each other, which means that they will often be created in the same direction.

When the cuts shown in table 1 are included, it appears the angular correlations are simply flattened. On average, the same limited number of particles will be formed on each side of the transverse plane. If, for example, a K^+ is formed on one side of the transverse plane, then, since another K^+ can not be formed on either side of the first K^+ , the number of possibilities of another K^+ on the same side of the transverse plane is decreased by three. This means that if another K^+ meson is formed in the same event as the first, then it is more likely to have formed on the other side of the transverse plane. The same reasoning applies to all four types of same-sign particle pairs, which explains why the correlation is higher around $\Delta\varphi = \pi$. Including cuts again simply flatten the correlation. The flattening that occurs when cuts are introduced is most likely due to the upper cut in p_T which removes the hard component of the jets, and only retains the softer and more smeared-out particles.

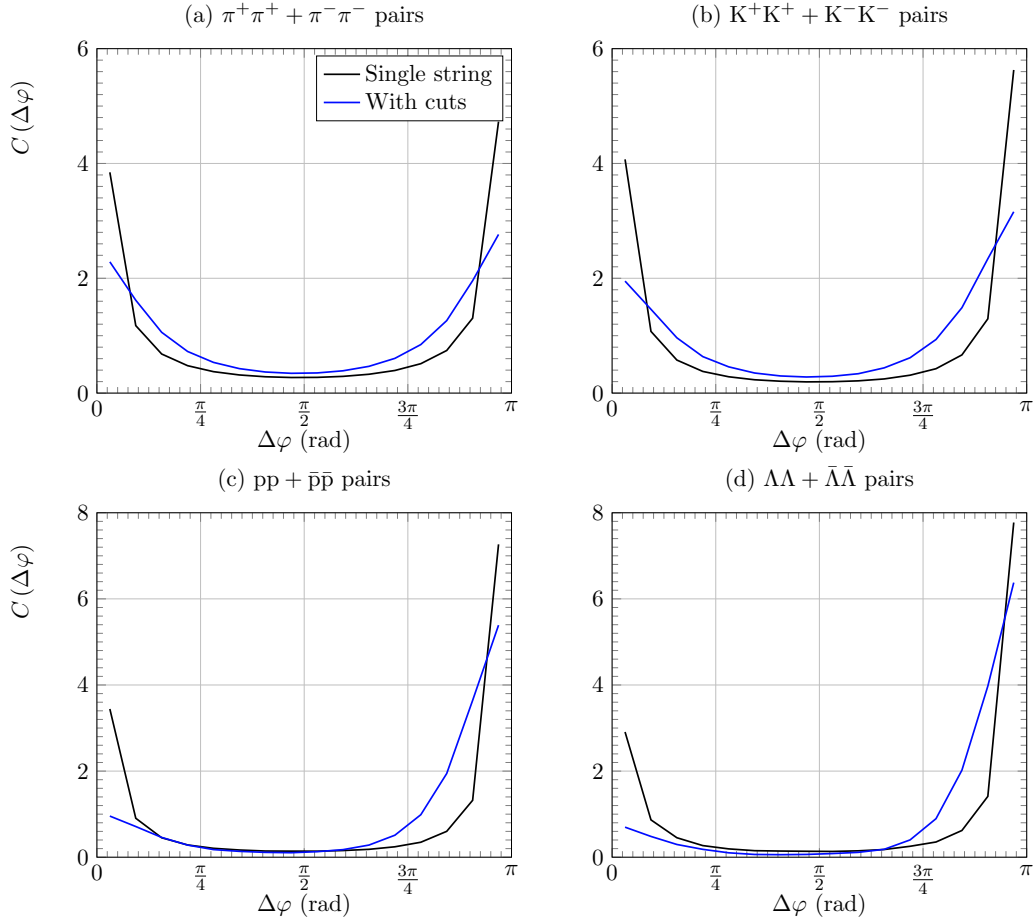


Figure 9: Angular correlations for same-sign particle pairs created from simple strings in the transverse plane.

5.2 Cuts and particle distributions

We here look at the particle distributions in η and p_T , as well as how the cuts in table 1 influence the angular correlations. The η distributions from inelastic pp collisions at $\sqrt{s} = 7$ TeV are shown in figure 10, where the red area shows the particles that are cut out according to the η cuts in table 1. We see that the cuts for η are quite restrictive. They reduce the sample to the lower end of the η spectrum.

We also notice that the pseudorapidity distributions are very similar for these four types of particles, except for the additional bump around $\eta = 8$ for both the protons and the Λ baryons which is likely related to diquark proton remnants which are likely to create protons and Λ baryons. The remnants often consist of a diquark made out of two of the three proton valence quarks, which means that there is only one possible slot a strange quark can fill to form a lambda baryon. Baryons created in other regions, however, have three possible slots a strange quark can fill to create a lambda baryon. This reasoning, although quite primitive, may explain why the bump around $\eta = 8$ is smaller for lambda baryons than for protons.

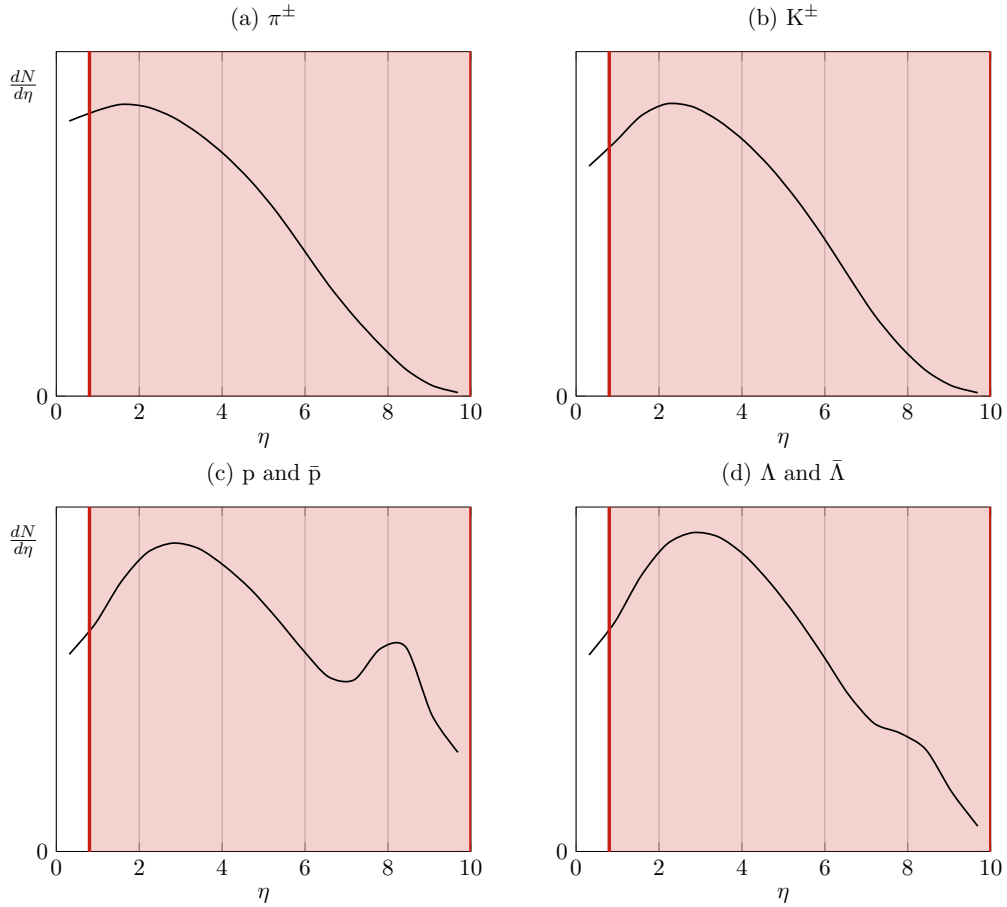


Figure 10: η distributions from pp collisions at $\sqrt{s} = 7$ TeV. All figures are shown with an arbitrary scale on the vertical axis. Excluded zones given in table 1 are marked in red.

The distributions of transverse momenta are shown in figure 11. These are the p_T distributions within the accepted η regions in figure 10. The p_T distributions look very similar even when the entire η spectrum is allowed, but these are not shown in the figure. We here see that the cuts imposed on transverse momenta are not as restrictive as the η cuts. All four types of particles share a similar distribution, but they appear to slightly depend on particle masses, which is not surprising. Only a small fraction of pions make it above 2 GeV, but there is a noticeable fraction of lambda baryons above 4 GeV.

We now, in figures 12 and 13, look at what correlations we can observe by completely removing any particle acceptance cuts, and by studying all inelastic events. If we compare the vertical scales in these figures with those in figures 4 and 5, we see that the correlations without cuts are smaller. This is because removal of cuts allows for an increased number of uncorrelated particles, e.g. a high rapidity particle that is unlikely to have formed in the same process next to a low rapidity particle.

Despite the flattening, we can still see some structure. The different-sign particle pairs have a tendency to be created right next to each other on a fragmenting string, which if they are cre-

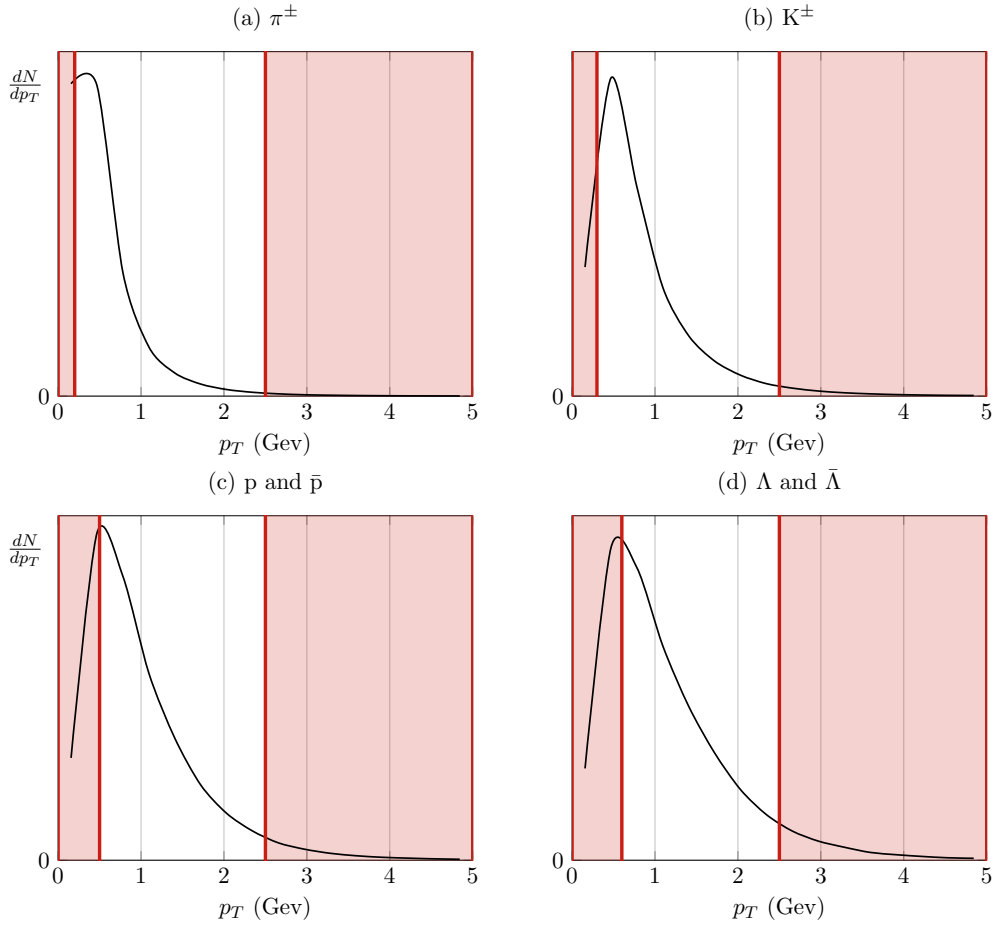


Figure 11: Corresponding p_T distributions within the specified η cuts. All figures are shown with an arbitrary scale on the vertical axis. Excluded zones given in table 1 are marked in red.

ated within a mini-jet explains the peak around $\Delta\varphi = 0$. For the different-sign pions, however, the peak around $\Delta\varphi = \pi$ appears to dominate. This is likely to be caused by the generally lower p_T for the pions, which implies that if a π^+ and a π^- are created next to each other on the string, then the opposite transverse kicks of the shared $q\bar{q}$ pair might be strong enough in relation to the pion mass to kick the two pions into opposite directions in the transverse plane.

The same-sign particle pairs all share a common correlation shape, with a dominating peak around $\Delta\varphi = \pi$. This is probably due to the limited number of particles that can form on a fragmenting string. If a proton is formed in one of two opposite jets, then another proton is slightly more likely to form in the opposite jet, as discussed previously in section 5.1.

5.3 Individual particle production mechanisms

This section concerns the effect of individual phenomena on the correlation function. Specifically, it shows how the correlation function is influenced by MPIs, ISR, FSR, primordial k_T , and decays. The correlation functions in this section, are all created by selecting particles according to the cuts specified in table 1, and are displayed, in relation to the “Baseline”

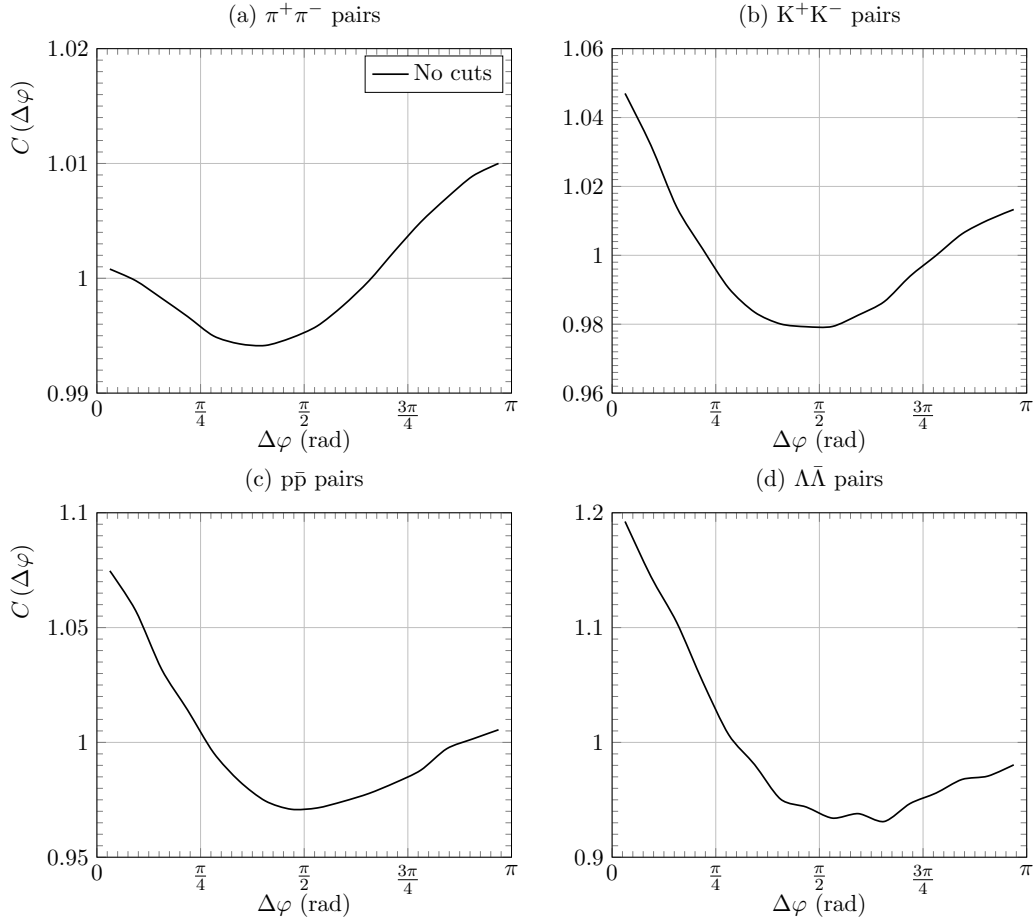


Figure 12: Angular correlations without acceptance cuts for different-sign particle pairs produced in pp collisions at $\sqrt{s} = 7$ TeV. Note the narrow range on the vertical scale.

and the experimental data, for different-sign particle pairs in figure 14, and are for same-sign particle pairs in figure 15.

In all eight subfigures it is clear that ISR and FSR have similar effects on the correlation function, which is that turning them off appears to amplify the magnitude of the correlation. This then means that the effect of keeping them on is to flatten the function, as discussed in section 3.1. A similar reasoning can be made for the MPIs, where we can also see that that the effect is generally stronger for the same-sign pairs.

The reason for this can be summed up in two key points. Firstly, as we have seen in section 5.2 concerning the effects of cuts, different-sign pairs are generally more likely to form next to each other and therefore often in the same mini-jet structure, while same-sign pairs are generally more likely to form in opposite mini-jets. Secondly, the jets may be longitudinally boosted, which means that two opposite jets might not be exactly opposite to each other in the laboratory frame. This leads to the possibility that they are not both entirely within the sample cuts, so that a majority of the particles accepted in an event are created in a single mini-jet, which would contribute to a peak around $\Delta\varphi = 0$ in the angular correlations.

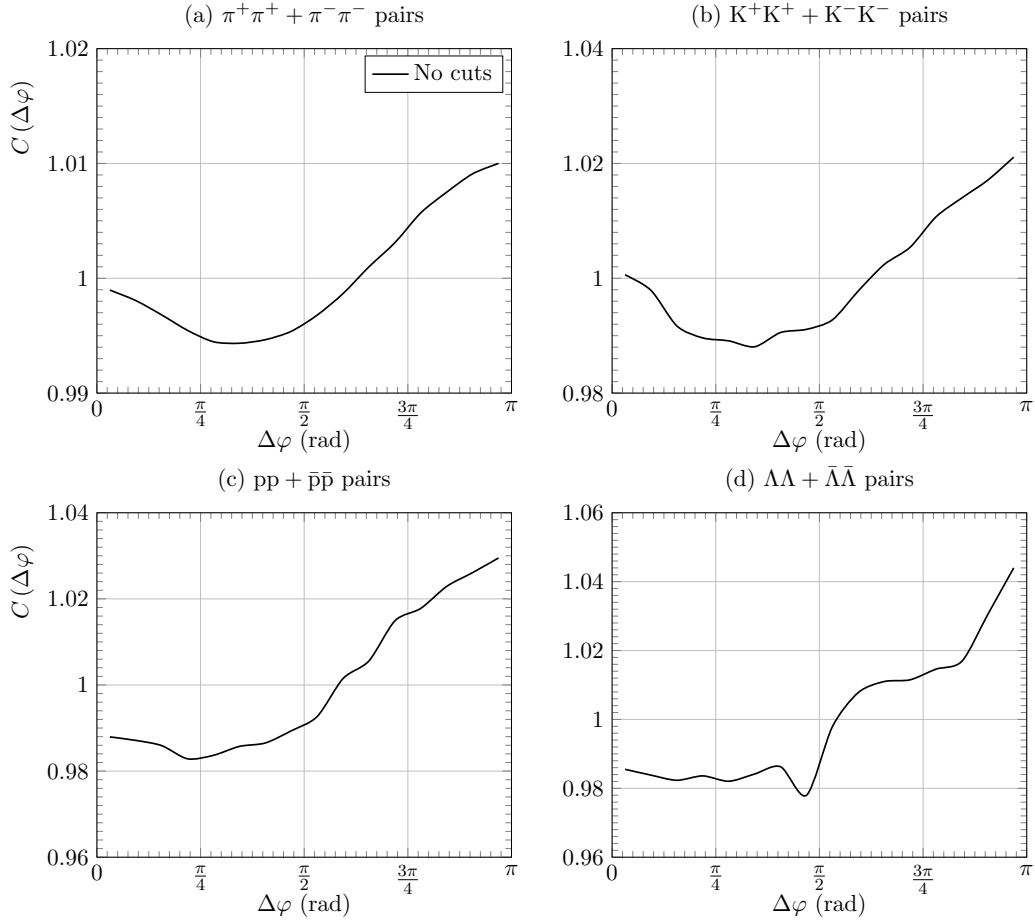


Figure 13: Angular correlations without acceptance cuts for same-sign particle pairs produced in pp collisions at $\sqrt{s} = 7$ TeV. Note the narrow range on the vertical scale.

Lastly, it is noted that both the effects of primordial transverse momentum and particle decays are quite small on the correlation function, except for the different-sign pions where there appears to be a significant amount of particles, such as the ρ^0 , which decays into a π^+ and a π^- with $\Delta\varphi \approx 0$.

6 Conclusions

ISR and FSR appear to both flatten the correlation function in the same way, and the flattening occurs for all types of particle pairs. This indicates that these types of radiation cause particles to be more spread out in the detector, as expected. MPIs also cause some flattening but in a slightly different way, as turning it off appears to highlight the particle pairs produced in a single mini-jet. The effect of primordial k_T on the correlation function appears to be insignificantly small for the cases discussed in this thesis. The effect of decays is generally more noticeable for mesons than baryons, since mesons are created in a large number of decays while baryons are more rare, but the effect is still relatively small.

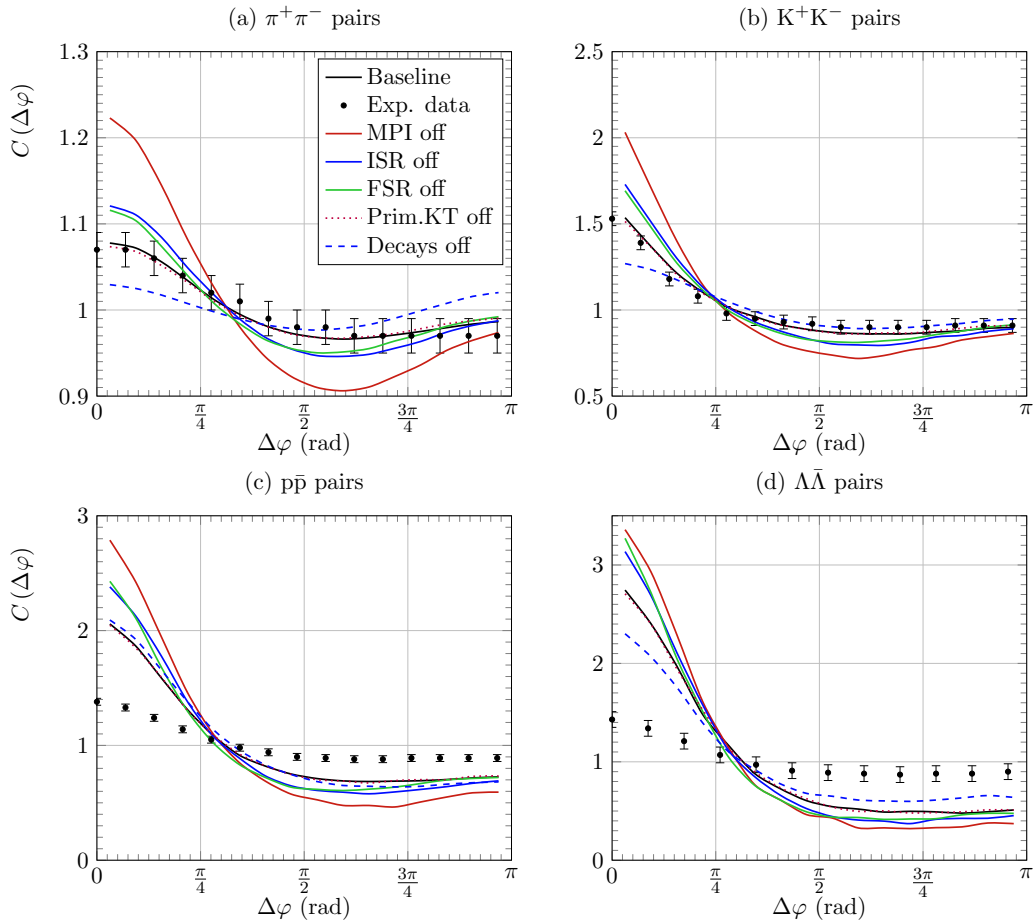


Figure 14: Angular correlations for different sign particle pairs produced in pp collisions at $\sqrt{s} = 7$ TeV and the effects of individual particle production mechanisms.

Unfortunately it isn't realistically possible to compare data from ALICE with PYTHIA simulations when any cuts are removed due to the difficulty of determining the particle type outside the specified η and p_T ranges. However, if possible, it might be good to analyse data from other detectors such as ATLAS or CMS to compare angular correlations with Monte Carlo event generators such as PYTHIA, within the limits where the detectors can identify particles with satisfactory accuracy.

The core of the problem seems to be that PYTHIA overestimates the number of baryons created in a single jet compared to complete events, leading to a correlation around $\Delta\varphi = 0$ which is larger than for experimental data. No obvious error in the particle production mechanisms studied in this thesis has been found. One possible solution to the problem may be to adjust PYTHIA's parameters that influence baryon production to better fit the experimental data. Another possibility might be to use a different model for baryon production, more on this can be found in ref. [6, 7].

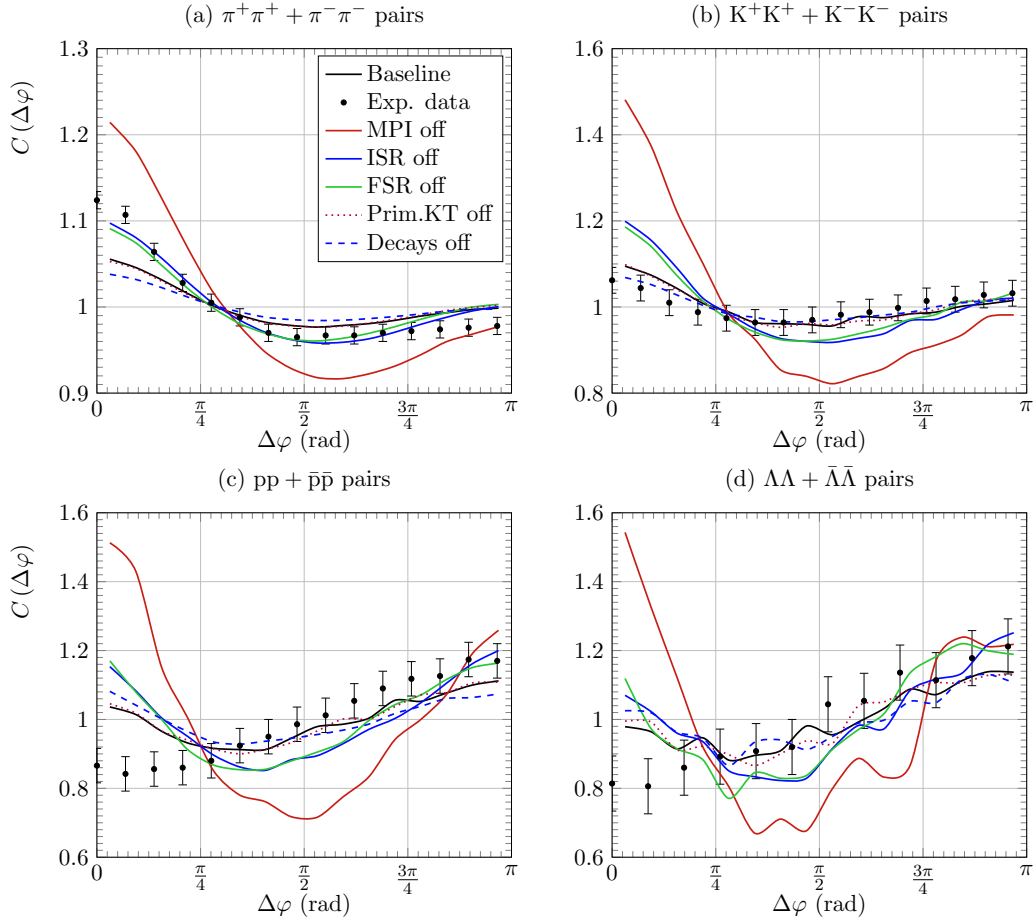


Figure 15: Angular correlations for same sign particle pairs produced in pp collisions at $\sqrt{s} = 7$ TeV and the effects of individual particle production mechanisms.

References

- [1] J. Adam *et al.* [ALICE Collaboration], “Insight into particle production mechanisms via angular correlations of identified particles in pp collisions at $\sqrt{s} = 7$ TeV,” arXiv:1612.08975 [nucl-ex].
- [2] J. Ellis, “TikZ-Feynman: Feynman diagrams with TikZ,” *Comput. Phys. Commun.* **210** (2017) 103 doi:10.1016/j.cpc.2016.08.019 [arXiv:1601.05437 [hep-ph]].
- [3] B. Andersson, G. Gustafson, G. Ingelman and T. Sjöstrand, “Parton Fragmentation and String Dynamics,” *Phys. Rept.* **97** (1983) 31. doi:10.1016/0370-1573(83)90080-7
- [4] T. Sjöstrand, “Monte Carlo Tools,” doi:10.1201/b11865-14 arXiv:0911.5286 [hep-ph].
- [5] T. Sjöstrand *et al.*, “An Introduction to PYTHIA 8.2,” *Comput. Phys. Commun.* **191** (2015) 159 doi:10.1016/j.cpc.2015.01.024 [arXiv:1410.3012 [hep-ph]].
- [6] B. Andersson, G. Gustafson and T. Sjöstrand, “Baryon Production in Jet Fragmentation and Υ Decay,” *Phys. Scripta* **32** (1985) 574. doi:10.1088/0031-8949/32/6/003

- [7] J. R. Christiansen and P. Z. Skands, “String Formation Beyond Leading Colour,” *JHEP* **1508** (2015) 003 doi:10.1007/JHEP08(2015)003 [arXiv:1505.01681 [hep-ph]].